Bio-Design and Manufacturing (2021) 4:441–451
https://doi.org/10.1007/s42242-021-00128-5

RESEARCH ARTICLE

# Adenosine-treated bioprinted muscle constructs prolong cell survival and improve tissue formation

**Dongxu Ke[1,2] · Adam M. Jorgensen[1] · Sang J. Lee[1] · James J. Yoo[1] · Sean V. Murphy[1]**

Received: 20 October 2020 / Accepted: 21 January 2021 / Published online: 12 February 2021


## Abstract

It is crucial to maintaining the viability of biofabricated human-sized tissues to ensure their successful survival and function after transplantation. Adenosine is a purine nucleoside that has the function to suppress cellular metabolism and has been previously proposed as a method to prolong cell viability under hypoxia. In this study, we optimized the dose concentration of adenosine for incorporation into bioprinted constructs to preserve long-term cell viability in vitro. Our results showed that muscle cells (C2C12) containing 6, 7, or 8 mM adenosine maintained high cell viability for 20 days under hypoxic conditions (0.1% $O_2$), whereas cells without adenosine treatment showed 100% cell death after 11 days. After 20 days under hypoxic conditions, muscle cells treated with adenosine proliferated and differentiated when transferred to normoxic conditions. From these adenosine concentrations, 6 mM was picked as the optimized adenosine concentration for further investigations due to its most effective results on improving cell viability. The bioprinted muscle constructs containing adenosine (6 mM) maintained high cell viability for 11 days under hypoxic conditions, while the control constructs without adenosine had no live cells. For in vivo validation, the bioprinted constructs with adenosine implanted under the dorsal subcutaneous space in mice, showed the enhanced formation of muscle tissue with minimal central necrosis and apoptosis, when compared to the constructs without adenosine. These positive in vitro and in vivo results demonstrate that the use of adenosine is an effective approach to preventing the challenge of hypoxia-induced necrosis in bioprinted tissues for clinical translation.

**Keywords** Bioprinting · Hypoxia · Adenosine · Cell viability · In vivo

## Introduction

Organ transplantation represents a significant advancement of modern medicine for treating organ failure due to diseases or injuries [1]. The medical practice of organ transplantation is mature; however, a major limitation is the donor organ shortage. In 2019, more than 113,000 people in the USA are on the organ transplant list; however, only 36,528 organ transplantations were performed [2]. Due to this mismatch, 20 people die each day in the USA waiting for organs for transplantation [2]. Besides the transplantation of entire organs, tissue substitutes are also in crucial need, especially for muscle substitutes. Volumetric muscle loss (VML) is a traumatic or surgical loss of skeletal muscle that requires muscle substitutes for regeneration. Traditionally, VML has been treated using autologous muscle flaps [3]. However, this procedure is inevitably associated with morbidity at the donor site and has limited successful outcomes, resulting in part from insufficient delivery of oxygen and nutrients to the site of injury [4].

Bioprinting is an emerging technology that has great potential to solve the challenge of limited organ supplies for transplantation. It has the advantage of being able to create complex 3D tissue structures with high resolution and designs based on each patient's needs [5–8]. Many tissues, including muscle, cartilage, and bone, and other complex tissues, such as trachea and meniscus, have been successfully bioprinted at small scales [9–15]. Recently, Choi et al. described a novel 3D bioprinting treatment for volumetric muscle loss. The constructs were composed of cell-laden dECM bioinks generated with a granule-based printing reservoir and coaxial nozzle printing to improve functional recovery of the constructs [16].

✉ Sean V. Murphy
semurphy@wakehealth.edu

[1] Wake Forest Institute for Regenerative Medicine, Wake Forest School of Medicine, Winston-Salem, NC, USA

[2] Novaprint Therapeutics Suzhou Co., Ltd, Suzhou, Jiangsu, China

However, several challenges need to be overcome for the translation of this technology to clinical applications. Bioprinted constructs require a vascular network to become mature and functionalized. The vascular network plays a crucial role in the body's metabolic system including the exchange of nutrients, oxygen, and waste among different tissues. Furthermore, the development of vascular networks is relatively slow [6, 17, 18]. It was reported that the average regeneration rate of microvessels was only around 5 μm per hour, so most human-sized tissues would require many weeks to become sufficiently vascularized [19, 20]. In current practice, by the time that a 3D bioprinted construct becomes vascularized, tissue necrosis is likely to occur due to a lack of oxygen and nutrient supply.

There have been some studies reporting the incorporation of vascular structures within the bioprinted construct to overcome this challenge. Dr. Lewis and her group developed thick vascularized tissues through bioprinting [21]. Bioprinted constructs with a thickness larger than 1 cm and a volume of 10 $cm^3$ were created with human mesenchymal stem cells (hMSCs), HNDFs, and vascular channels produced by Pluronic F127. Results showed high cell viability for cells close to vascular channels, successful lumen formation within the area of vascular channels, and the differentiation of hMSCs toward osteoblasts after 45 days of culture. However, they found that cells far from bioprinted vascular channels still died due to a lack of oxygen and nutrient during culture. Thus, even with current success, bioprinted tissues are far from clinical translation. This is because creating complex vascular structures including microvasculature (up to 2 mm in diameter), intermediate microvessels (50–500 μm in diameter), and capillary networks (10–20 μm in diameter) within bioprinted tissues in a short time is still a major challenge [22].

The best way to develop vascularized tissues is still through self-vascularization within bioprinted tissue constructs. However, tissue necrosis often occurs during the vascularization process due to an insufficient oxygen supply. An approach to increasing the long-term cell viability of bioprinted tissue constructs under hypoxic conditions is promising to achieve this goal. Adenosine is a purine nucleoside that has the function of an energy transferring molecule [23, 24]. It has been reported to play a crucial role in decreasing neuronal excitability as well as neurotransmitter release resulting in effectively reduced neuronal energy requirements [25]. The angiogenesis in bioprinted tissue constructs is a long-term process. Providing sufficient oxygen and nutrients for bioprinted tissues until vascular formation has been a major challenge. One potential approach to overcoming this challenge is to add adenosine to bioinks for the preparation of bioprinted tissues. With the effects of adenosine on downregulating the cellular metabolic activity, the requirement of oxygen and nutrient for cellular survival will be significantly decreased in bioprinted tissue constructs, which is promising to enhance the cell viability during the vascularization process.

In this study, our overall hypothesis is that the downregulation of cell metabolism through treatment with adenosine should improve the viability of bioprinted constructs. To test our hypothesis, we first optimized the concentration of adenosine to achieve long-term cell viability under 0.1% $O_2$ hypoxic conditions to mimic a harsher than expected cellular hypoxic condition prior to angiogenesis of bioprinted tissue constructs. After 20 days, samples were transferred from hypoxic to normoxic conditions to evaluate maintenance of cellular viability and metabolism. One concentration with the best cellular viability, metabolism, and differentiation will be selected as the optimized concentration of adenosine. This concentration should be expected to be appropriate for further application. Then, adenosine was incorporated into our cell-laden fibrinogen-based bioinks, followed by the fabrication of muscle constructs using the WFRIM Integrated Tissue Organ Printer (ITOP) [12]. Bioprinted muscle constructs were cultured under hypoxic conditions and characterized through live/dead staining and MTT cell proliferation assay. Additionally, bioprinted muscle constructs were implanted under the dorsal subcutaneous space in mice for two weeks to study the effects of adenosine on cell viability and muscle formation through histological and immunohistochemical analysis.

## Materials and methods

### Materials

All chemicals that were not mentioned particularly in this study were purchased from Sigma-Aldrich (St. Louis, MO).

### In vitro 2D culture

A mouse skeletal muscle cell line, C2C12 (ATCC® CRL-1772™, ATCC, Manassas, VI), was used in this study. In total, 20,000 cells were seeded in each well of 24-well plates with 1 mL C2C12 growth medium containing Dulbecco's Modified Eagle Medium (DMEM) high glucose medium, 10% FBS, and 1% penicillin and cultured under normoxic conditions (37 °C and 5% $CO_2$) for one day to allow their attachment. Then, the medium was aspirated and filled with 1 mL of fresh C2C12 growth medium with either 0 (control), 5, 6, 7, or 8 mM adenosine ($n=3$). Cultures were maintained under 0.1% $O_2$ hypoxic conditions for up to 20 days without medium change. This setup was to mimic the expected tissue microenvironment after construct implantation prior to vascularization, when there was no vascular structure for the

transportation of oxygen, nutrients, and cellular metabolites between tissues and outside environment.

After 20 days, five samples from each adenosine group were transferred from hypoxic to normoxic conditions when they still had cellular viability and metabolism. This experimental approach transferring cultures from hypoxic to normoxic conditions was designed to model the expected conditions experienced by a construct after implantation and prior to angiogenesis, and then for the evaluation of function after vascularization. They were changed with a fresh C2C12 growth medium every other day till day 25. Then, C2C12 differentiation medium containing Dulbecco's Modified Eagle Medium/Nutrient Mixture F-12 (DMEM/F12), 1% horse serum, and 1% penicillin was changed for these samples every other day until day 28. These samples were evaluated for muscle differentiation. The timeline of in vitro 2D culture is shown in Fig. 1(a).

## Bioink preparation

Three bioinks were used in this study. Bioink 1 was constituted of 40 mg/mL fibrinogen, 45 mg/mL gelatin, 3 mg/mL hyaluronic acid (HA), and 10% v/v glycerol in DMEM high glucose medium. Bioink 2 had the same composition as bioink 1, with additional supplementation with 30 mM adenosine. Bioink 3 also had a similar composition to bioink 1, while it had no fibrinogen. Adenosine was first dissolved in DMEM high glucose medium at 37 °C through a rotary mixer at 50 rpm for 1 h. Then, HA and glycerol were added to the solution and mixed under the same condition overnight. After that, gelatin and fibrinogen were added and mixed under the same condition for 2 h. Finally, all bioinks were sterilized by filtering using a 0.4 μm filter before bioprinting.

## In vitro 3D culture of bioprinted muscle constructs

Bioprinting was conducted using the Wake Forest Institute of Regenerative Medicine Integrated Tissue Organ Printer (ITOP) [12]. This is an extrusion-based bioprinting system with six separate bioink-dispensing lines. Both polycaprolactone (PCL) and bioinks were used for the bioprinting of muscle constructs. Two designs were used in this study, as shown in Figs. 4(b) and 5(a). For in vitro experiments, design 1 [Fig. 4(b)] with a dimension of $10 \times 10 \times 0.5$ mm was used, while design 2 [Fig. 5(a)] with a dimension of $12 \times 12 \times 4.5$ mm was used for in vivo experiments. Green indicates PCL, red indicates bioink 1 or 2, and blue indicates bioink 3. Samples printed with bioink 1 are labeled control, while samples printed with bioink 2 are labeled 30 mM AD. Before bioprinting, 25 million C2C12 cells were laden in 1 mL of each bioink. PCL was heated to 90 °C and dispensed using a 200 μm metal nozzle at 700 psi. All bioinks were used at 15 °C and dispensed using a 200 μm Teflon nozzle at 150 psi. After the bioprinting was complete, constructs were cross-linked by immersion into 20 UI/ml thrombin solution for 1 h. Then, samples with design 1 were filled with C2C12 growth medium and cultured under 0.1% $O_2$ hypoxic conditions for up to 15 days without medium change for in vitro characterization. In addition, five samples from each group were transferred from hypoxic to normoxic conditions at day 11 when they were still viable and metabolizing. They were cultured in normoxic conditions until day 15. Samples with design 2 were also filled with C2C12 growth medium, while they were cultured in normoxic conditions (37 °C and 5% $CO_2$) for one day before in vivo implantation. The timeline of in vitro 3D culture is shown in Fig. 4(a).

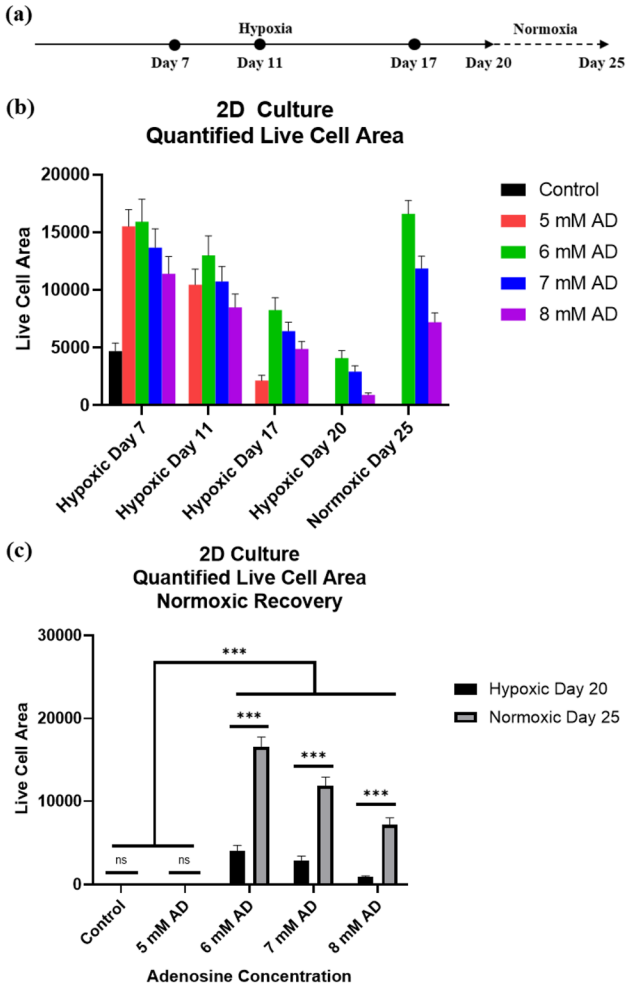


**Fig. 1** **a** Schematic of 2D culture time points and conditions. **b** Live cell area calculated based on live/dead assays with the addition of 0 (hypoxic control), 5, 6, 7, 8 mM adenosine for 7, 11, 17, 20, and 25 days under 0.1% $O_2$ hypoxic conditions or normoxic conditions. **c** Live cell area calculated based on live/dead assays between different compositions at day 20 and day 25

## Live/dead staining

An Early Tox Live/Dead Assay Kit (Molecular Devices, San Jose, CA) was used for 2D culture in well plates following the manufacturer-recommended protocol to observe the cell viability of C2C12 cells. Cell-permeant red dye could bind to the DNA of all cells, while green dye could only react to dead cells without membrane integrity giving them yellow fluorescence. Briefly, red and green dyes were 1:2000 diluted with Dulbecco's phosphate-buffered saline (DPBS) as the working solution and then added to each well. After incubation at 37 °C and 5% $CO_2$ for 20 min, fluorescence images were taken using Spectra Max i3x with MiniMax 300 Imaging Cytometer (Molecular Devices, San Jose, CA) using the setup of excitation and emission provided in the SoftMax Pro 7.0.2 (Molecular Devices, San Jose, CA). Then, the cell area was calculated for each composition using Image J. The cell area was used to indicate the cell viability during 2D culture since dead cells often detach from the bottom surface. This area was selected by choosing an appropriate threshold without losing signals and fusing cells close to each other. Additionally, five images were used for the quantification of cell viability to ensure the reproducibility of data.

For 3D culture using bioprinted muscle constructs, 2 μM calcein AM and 4 μM Ethidium homodimer-1 (EthD-1) solution was prepared using stock solutions from LIVE/DEAD® Viability/Cytotoxicity Kit (Thermal Fisher Scientific, Waltham, MA) and added to the constructs to fully cover them. After incubation at room temperature for 30 min, an Olympus BX63 fluorescence microscope was used to take images of bioprinted muscle constructs. Green was changed to red and red was changed to green, consistent with the live/dead images of 2D culture in well plates. In addition, Image J was used to quantify cell viability based on these images. Cell viability percentage was calculated as the area of red (live cells) divided by the area of red and green (total cells) ($n = 3$).

## Cell proliferation

A 3-(4,5-dimethylthiazol-2-yl)-2,5-diphenyl tetrazolium bromide (MTT) assay (Sigma, MO, USA) was used to evaluate the cell proliferation. MTT assay solution was prepared by adding 50 mg of MTT powder into 10 ml phosphate-buffered saline (PBS) followed by sterilization using 0.45 μm filters. Nine hundred microliters of cell medium and 100 μl of MTT solution were added separately to each sample. Then, samples were incubated at 37 °C for 2 h. After incubation, the MTT solution was removed and 500 μl of dimethyl sulfoxide (DMSO) was added to each sample. After pipet mixing, 100 μl solution was transferred into each well of 96-well plates and read by a Spectra Max i3x microplate reader at 570 nm. Three duplicates were tested for each composition to ensure reproducibility.

## Muscle differentiation test

Samples were fixed in 4% paraformaldehyde (PFA) in PBS solution for 10 min. After that, they were permeabilized with 0.1% Triton X-100 in PBS solution for 10 min. Then, they were blocked with a protein block solution (Dako, Carpinteria, CA) for 30 min. The primary antibody, Myosin 4 Monoclonal Antibody (MF20) (14-6503-80, Thermo Fisher Scientific, Waltham, MA) (1:300 dilution), was applied on samples at room temperature for 1 h. After washing by PBS five times, the secondary antibody, goat anti-mouse IgG (H + L) secondary antibody Alexa Fluor 594 (A-11005, Thermo Fisher Scientific, Waltham, MA) (1:300 dilution), was applied on samples for 40 min with aluminum foil covered to avoid light exposure. After five times of PBS wash, DAPI counterstain (1:1000 dilution) was applied on samples for 5 min. After another five times of PBS wash, 4% PFA in PBS solution was used to fix the stain. Then, immunofluorescence images were taken using an Olympus BX63 fluorescence microscope.

## Implantation of bioprinted muscle constructs

Animal care, housing, and procedures were performed in accordance with the protocol approved by the Animal Care and Use Committee of Wake Forest Institute of Regenerative Medicine. A total of four nude mice were distributed into two experimental groups: control group—bioprinted muscle constructs using PCL and bioink 1, and 30 mM AD group—bioprinted muscle constructs using PCL and bioink 2. One control group construct and one 30 mM AD group construct were implanted into the left and right dorsal subcutaneous spaces of each nude mouse. All mice were killed after two weeks of implantation.

## Histological analysis

Two weeks postimplantation, mice were euthanized to retrieve samples. Retrieved implants were fixed in 10% Neutral buffered formalin (NBF) overnight followed by a dehydration process. Then, they were embedded in paraffin wax and sectioned by a microtome to a thickness of 5 μm. Sections used for the staining were close to the center of bioprinted constructs. Tissue sections were deparaffinized and then stained with hematoxylin and eosin (H&E) to examine the tissue formation within bioprinted muscle constructs. Bright-field images were taken using an upright microscope (Olympus BX63, Tokyo, Japan).

### Immunohistochemistry analysis

Sections were first deparaffinized and rehydrated followed by antigen retrieval procedures at pH 6. Then, samples were incubated in Peroxiblock (Dako, Carpinteria, CA) for 20 min. After washing with Tris-buffered Saline with Tween 20 (TBST) three times, samples were further incubated in protein block solution (Dako, Carpinteria, CA) for another 20 min. Sections were then incubated with Anti-HIF-1 alpha antibody (HIF1A) (ab1, Abcam, Cambridge, MA) (1:200 dilution) and anti-desmin antibody (desmin) (ab15200, Abcam, Cambridge, MA) (1:200 dilution) at 4 °C overnight and rinsed three times with TBST afterward. After that, sections were incubated with biotinylated secondary antibody, goat anti-rabbit/mouse IgG (H + L) (Vector Laboratories, Burlingame, CA, USA), at room temperature for 30 min. Then, they were rinsed three times with TBST and an avidin-biotinylated horseradish peroxidase complex (Vector Laboratories, Burlingame, CA, USA) was applied at room temperature for 30 min. Sections were rinsed three times with TBST and 3,3′-diaminobenzidine solution (Vector Laboratories, Burlingame, CA, USA) was applied. When the color change was seen under the microscope, samples were immediately immersed into water to stop the reaction. Finally, sections were counterstained with Gill's hematoxylin and mounted with a mounting solution. Images were taken using a light microscope (Leica, DM 400B, Wetzlar, Germany) with digital imaging software (Pro Express 6.3 software).

### Statistical analysis

Data were expressed for each experimental group as mean ± SD and statistical significance determined using statistical analysis software (GraphPad Prism, GraphPad Software Inc.). Mixed models analysis of variance techniques were used to compare outcomes. Models included the factors TREATMENT, DAY, and a TREATMENT x DAY interaction. A confidence interval of 95% assumes significance ($n = 3$).

## Results

### 2D cell viability and metabolism

For further analysis, 7, 11, 17, 20, and 25 days were picked since these five time points best reflected the changes of samples during 2D in vitro culture. For day points between 11 and 17, such as day 14, the changes of cell metabolism for all samples were not significant, so they were not further analyzed. Meanwhile, at day 20, we observed a significant loss of cell viability for all samples, so we decided to set day 20 as the endpoint for hypoxic cell culture. A live/dead assay was used for 2D culture to observe the cell viability of C2C12 cells. Control samples show a large number of dead cells by day 7, compared with a higher level of viability in samples treated with adenosine [4690 ± 707 (control) versus 15,502 ± 1481 (5 mM AD), 15,915 ± 1941 (6 mM AD), 13,680 ± 1635 (7 mM AD), 11,402 ± 1492 (8 mM AD), respectively, measured in pixels per area], as shown in Fig. 1(b) and (c). By day 11, there was no cell viability in the control group, and cells were detached, while adenosine-treated groups maintained high viability [2 ± 0.23 (control) versus 10,453 ± 1357 (5 mM), 12,996 ± 1693 (6 mM), 10,749 ± 1290 (7 mM), 8494 ± 1144 (8 mM), respectively, measured in pixels per area]. On day 17, samples with 5 mM adenosine began to display altered morphology and detach, while all other adenosine groups demonstrated a slight decrease in viability. At day 20, cells in samples with 5 mM adenosine were dead and detached (20 ± 3.6, measured in pixels per area). Cells treated with 6 mM adenosine show the highest viability, with a trend toward decreased viability in samples treated with 7 mM and 8 mM [4088 ± 651 (6 mM AD) versus 2932 ± 498 (7 mM AD), 909 ± 158 (8 mM AD), respectively, measured in pixels per area]. Following measurement at day 20, samples were cultured for 5 days in normoxic conditions. Samples treated with 6, 7, and 8 mM adenosine had increased viability, suggesting cell proliferation, with the greatest increase in viability (from 4088 ± 651 to 16,597 ± 1163 measured in pixels per area) seen in samples treated with 6 mM adenosine. Alternatively, untreated samples and those treated with 5 mM adenosine show no significant proliferation between day 20 and day 25, as shown in Fig. 1(b).

MTT assays were performed to evaluate cell metabolism in the presence or absence of adenosine. All groups show high cell metabolism at day 7, with 5 mM adenosine and untreated controls having the highest MTT [0.57 ± 0.02 (5 mM AD) and 0.53 ± 0.02 (control)], as shown in Fig. 2(a). By day 11, there is a trend toward decreased MTT, with the nontreated control having significantly less MTT than adenosine-treated groups [0.04 ± 0.001 (control) versus 0.40 ± 0.02 (5 mM AD), 0.33 ± 0.03 (6 mM AD), 0.26 ± 0.02 (7 mM AD), and 0.24 ± 0.01 (8 mM AD), respectively]. This trend continues at day 17, with all adenosine groups still having significantly higher MTT than the control [0.04 ± 0.001 (control) versus 0.08 ± 0.01 (5 mM AD), 0.27 ± 0.04 (6 mM AD), 0.26 ± 0.02 (7 mM AD), and 0.23 ± 0.03 (8 mM AD), respectively], at which time the MTT level of samples treated with 6, 7, and 8 mM adenosine only shows slight decreases from day 11, while samples with 5 mM adenosine show a significant decrease in MTT (from 0.39 ± 0.02 to 0.08 ± 0.01). By day 20, the MTT of all adenosine groups continues to decrease, with samples treated with 5 mM adenosine having almost no MTT value,

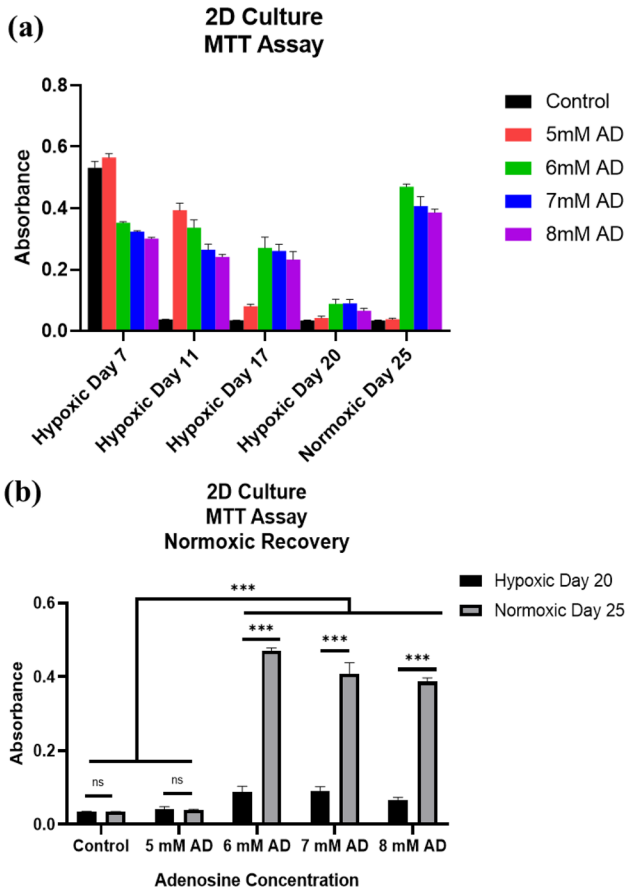


**Fig. 2** **a** MTT assay of C2C12 cells cultured under 0.1% $O_2$ hypoxic conditions or normoxic conditions with the addition of 0 (hypoxic control), 5, 6, 7, 8 mM adenosine for 7, 11, 17, 20, and 25 days. **b** MTT assay between different compositions at day 20 and day 25

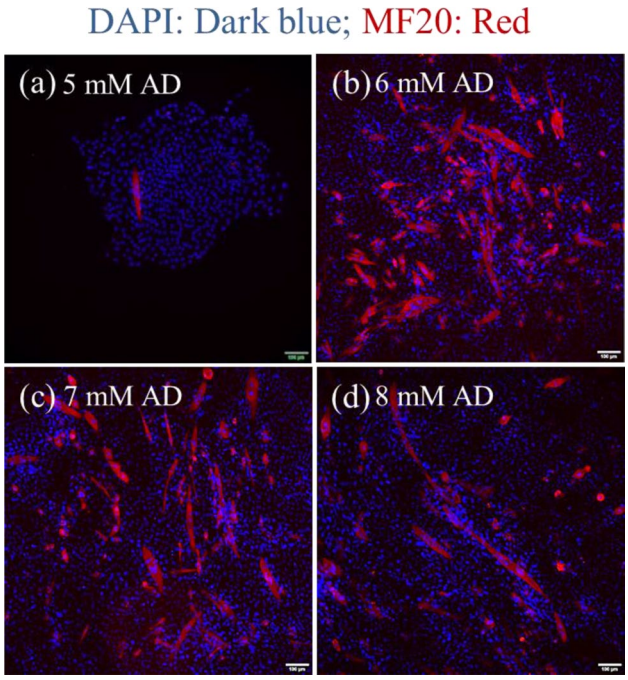


**Fig. 3** Florescence images of myotubes through MF20 staining for samples cultured with 5 mM (**a**), 6 mM (**b**), 7 mM (**c**), and 8 mM (**d**) of adenosine

comparable to the nontreated controls [0.04 ± 0.001 (5 mM AD) versus 0.04 ± 0.01 (control)], while 6, 7, and 8 mM adenosine-treated samples still maintain higher MTT values (0.08 ± 0.02 (6 mM AD), 0.09 ± 0.01 (7 mM AD), and 0.07 ± 0.01 (8 mM AD), respectively). When samples were transferred back to normoxic conditions at day 20 followed by culturing normoxic culture for 5 days, samples treated with 6, 7, and 8 mM adenosine had significantly increased MTT [0.47 ± 0.01 (6 mM AD), 0.41 ± 0.03 (7 mM AD), and 0.39 ± 0.01 (8 mM AD), respectively]. The increase between day 20 and day 25 is most striking for samples treated with 6 mM adenosine, which is close to four times increase (from 0.09 ± 0.02 to 0.47 ± 0.01). Samples treated with 5 mM adenosine and nontreated controls continue to have low MTT on day 25, as shown in Fig. 2(b).

## 2D cell differentiation

MF20 staining was conducted to evaluate cell differentiation when transferring from hypoxic to normoxic conditions. It shows that samples with 5 mM adenosine do not show obvious signs of cell differentiation, as shown in Fig. 3(a); however, samples with 6, 7, and 8 mM adenosine show positive staining of myotubes, as shown in Fig. 3(b), (c), and (d), especially for samples with 6 mM adenosine, as shown in Fig. 3(b).

## 3D cell viability and metabolism

A live/dead assay was used for 3D culture to observe the cell viability of bioprinted constructs under hypoxic conditions. Both 30 mM AD and no treatment control groups show high cell viability at day 7 [98% ± 0.5 (30 mM AD) and 97% ± 0.2 (control)], as shown in Fig. 4(c), (d), and (e). Cell death is observed in both groups at day 11; however, the 30 mM AD group has more live cells than the control [75% ± 6 (30 mM AD) versus 17% ± 2 (control), $p < 0.0001$]. By day 15 under hypoxic conditions, 30 mM AD group showed reduced cell viability but still maintained more viable cells than no-treatment controls**.** This drop was likely due to the effects of long-time hypoxia on reducing cell viability. When transferring samples from hypoxic to normoxic conditions at day 11 followed by 4 days of normoxic culture, 30 mM AD group shows a significant increase in cell viability (from 75% ± 6 to 98% ± 0.1). This cell proliferation through the increased number of live cells is in stark contrast with the no treatment control group, which has no significant increase in

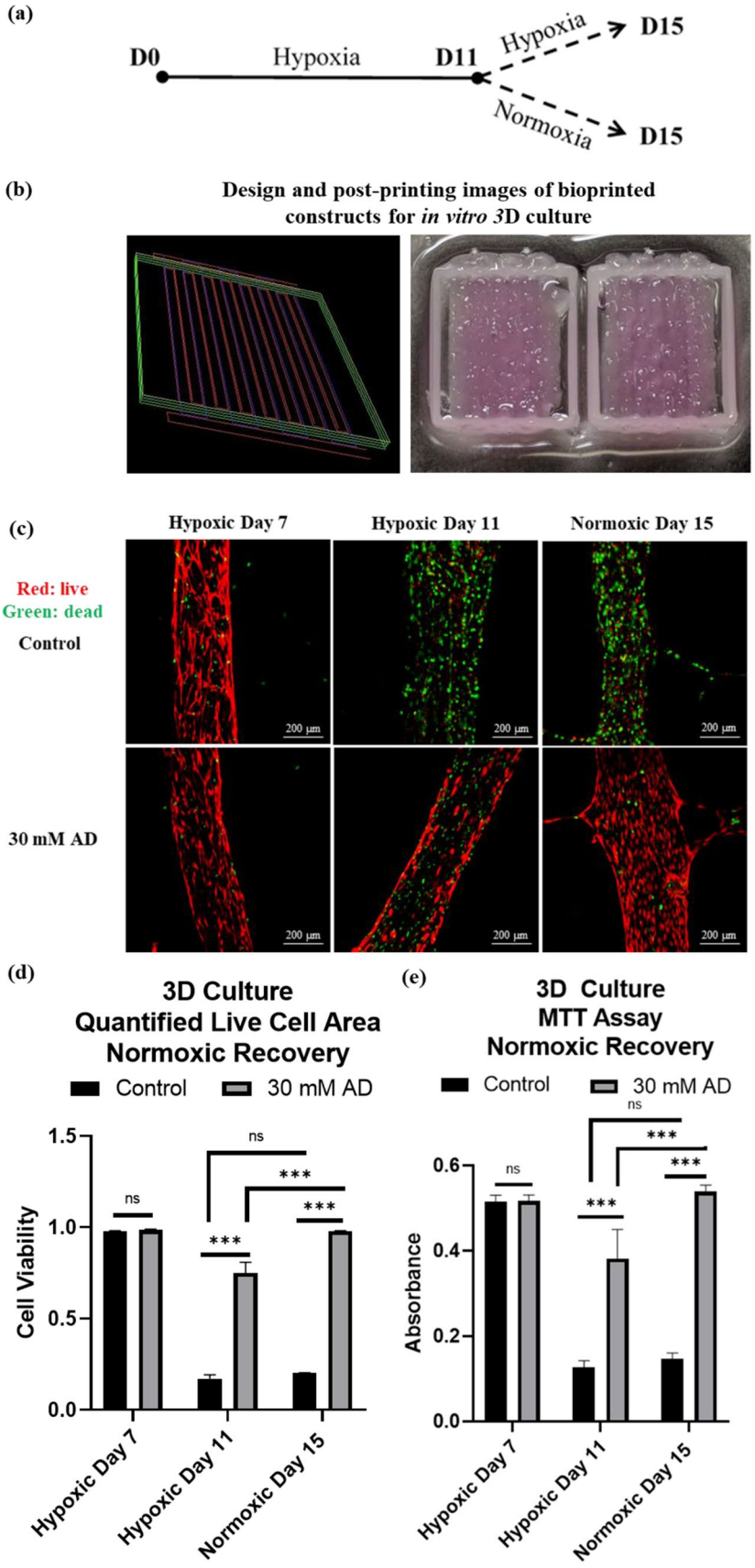


**Fig. 4** **a** Schematic of 3D culture time points and conditions. **b** Designs and post-printing images of bioprinted constructs for in vitro 3D culture. **c** Live/dead staining of bioprinted muscle constructs using fibrinogen-based control and 30 mM AD bioinks cultured under 0.1% $O_2$ hypoxic conditions or normoxic conditions for 7, 11, and 15 days (red: live; green: dead). **d** Live cells calculated based on live/dead images using Image J. **e** MTT assay of bioprinted muscle constructs during the culture

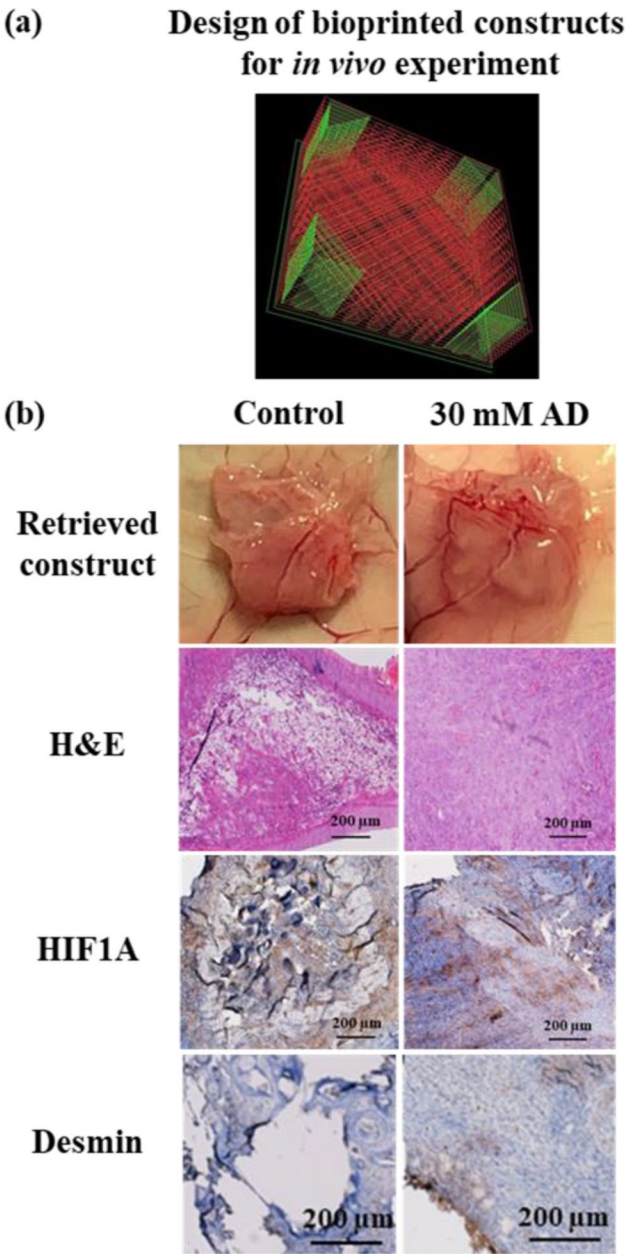


**Fig. 5** **a** Designs of bioprinted muscle constructs for in vivo experiment **b** Images of retrieved constructs, H&E staining, HIF1A staining, and desmin staining using bioprinted control muscle constructs and bioprinted 30 mM AD muscle constructs after implantation in dorsal subcutaneous spaces of mice for two weeks

viability after four days in normoxic culture (from 17% ± 2 to 20% ± 0.3), as shown in Fig. 4(c) and (d). These results correlate with our previous findings showing the effects of adenosine on increasing the cell viability under hypoxic conditions and maintaining the ability to reproliferate when transferred back to normoxic conditions.

Then, MTT assays were performed to evaluate cell metabolism of bioprinted constructs when adenosine was added. Control and 30 mM AD groups have comparable MTT metabolism at day 7 [0.52 ± 0.02 (30 mM AD) versus 0.52 ± 0.01 (control)], as shown in Fig. 4(e). Both groups show decreased MTT at day 11, while 30 mM AD group has significantly higher MTT than the control [0.38 ± 0.07 (30 mM AD) versus 0.13 ± 0.02 (control)]. At day 15 under sustained hypoxia, both 30 mM and nontreated control groups show decreased MTT compared to day 11 and their MTT values are comparable. When transferring both groups back to normoxic conditions at day 11 followed by culturing for 4 days in normoxic conditions, the 30 mM AD group shows increased MTT (from 0.38 ± 0.07 to 0.54 ± 0.02). Alternatively, the nontreated control group had no significant increase in MTT following 4 days of normoxic culture (from 0.13 ± 0.02 to 0.15 ± 0.01). The final MTT in the 30 mM AD group at day 15 is also significantly higher than in the nontreated controls [0.54 ± 0.02 (30 mM AD) versus 0.15 ± 0.01 (control)].

## Histological analysis

For in vivo characterizations using bioprinted constructs implanted in mouse dorsal subcutaneous spaces, there are no obvious visual differences between control and 30 mM AD groups when retrieving them after two weeks of implantation. Holes from the four corners might be caused by the presence of PCL near corner positions. Hydrogels show little degradation after two weeks of implantation. H&E-stained images from the control group show central disintegration indicating its apoptosis in the center, while the 30 mM AD group has intact and healthy tissue formation in their center, as shown in Fig. 5(b).

## Immunohistochemical analysis

For in vivo immunohistochemical analysis of bioprinted constructs, two stainings are used in this study. H1F1A is used to detect the hypoxic response of cells within the construct, while desmin is used as the marker of the C2C12 differentiation. For H1F1A staining, a large amount of positive HIF1A staining is observed in the center of bioprinted constructs from the control group; however, 30 mM AD group shows much less HIF1A expression compared to the control. For desmin-stained images, we detect the disintegration near the center area of bioprinted constructs in the control group indicating apoptosis, which corresponds to H&E-stained images; however, this observation is not seen in 30 mM AD group. Positive desmin staining is found mostly near the edge of bioprinted constructs; however, the center of bioprinted constructs from the 30 mM AD group also presents positive desmin staining, as shown in Fig. 5(b).

## Discussion

Tissue vascularization is crucial to the future clinical translation of bioprinted tissues; however, the vascularization of a human-sized tissue can take several months leading to tissue necrosis in the center of bioprinted tissue due to hypoxia [6, 26]. The goal of this study is to alleviate the effects of hypoxia on cell viability through the incorporation of adenosine, which should help maintain the cell viability before vascularization. In this study, we used a harsh oxygen environment, 0.1% $O_2$, to simulate the hypoxic conditions in vitro. In real cases, the oxygen level in the center of bioprinted tissues should be higher. Hence, we should expect the superior effects of adenosine on improving cell viability than our current results. In addition, in our in vitro 2D and 3D experiments, we selected the longest time points that all samples still have cell viability and metabolism under hypoxia to reproliferate and differentiate them under normoxia to further optimize the adenosine concentration.

Four concentrations of adenosine, 5, 6, 7, and 8 mM, are tested for optimization first. High cell viability can be maintained for up to 20 days by using 6, 7, and 8 mM adenosine; however, control samples and samples with 5 mM adenosine showed complete cell death and cellular detachment after 11 and 20 days, respectively, as shown in Fig. 1. The MTT result correlates with our previous findings showing significantly higher MTT at day 11, 15, and 20 for samples with 6, 7, and 8 mM adenosine compared to the control, while control samples and samples with 5 mM adenosine start to show substantially decreased MTT level after 11 and 20 days of culture, respectively, as shown in Fig. 2. Our results also correlate with a previous study showing the presence of adenosine enhances the cell viability for 11 days; however, our study extends this period to 20 days [23]. In addition, cell proliferation and differentiation tests are conducted after transferring samples from hypoxic to normoxic conditions. Samples with 6, 7, and 8 mM adenosine show enhanced cell viability and a significantly higher proliferation rate than the control after culturing at normoxic conditions for 5 days. They also demonstrate evenly distributed myotube formation through MF20 staining, while samples with 5 mM adenosine show little myotube formation, as shown in Fig. 3. Finally, 6 mM is picked as the optimal concentration of adenosine based on its highest cell viability and proliferation under hypoxic conditions as well as the most improved proliferation and differentiation when transferred back to normoxic conditions.

The next step is to add our optimal concentration of adenosine to bioprinted tissues and test them in vitro and in vivo. For in vitro characterizations, a design with two layers of muscle fibers is used, as shown in Fig. 4(b). PCL (green) is used as the mechanical support, while bioinks 1 and 2 (red) are fibrinogen-based bioinks, which have been reported to be biocompatible and support the muscle formation [27–29]. Bioink 3 is used as the sacrificial bioink and has a similar composition to bioink 1, while it has no fibrinogen. The function of bioink 3 is to provide temporary structural support to the construct at room temperature during the bioprinting process, while it can be easily removed at 37 °C post-printing during tissue culture. As we transitioned from in vitro analysis to our in vivo model, we aimed to keep the adenosine concentration in bioink 2 similar to in vitro experiments controlled for cell density (equal amounts of adenosine per cell). However, there were several practical limitations on the maximal dose we could include in our constructs. First, the maximum recommended clinical maximum dose for adult or pediatric patients is 12 mg/mL (45 mM). Second, due to the high cell density and bioink material properties, we began approaching the upper limit of solubility of adenosine in our materials. For this reason, 30 mM adenosine appeared to be a suitable concentration in bioink 2 without altering bioink material properties or limiting potential clinical applications.

Results show similar cell viability and proliferation between bioprinted control and 30 mM AD tissues under hypoxic conditions on day 7. Both groups experience a decrease in cell viability and proliferation at day 11 and 15, while the 30 mM AD group shows a less decrease than the control, as shown in Fig. 4(c–e). In addition, 30 mM AD group reproliferates substantially faster than the control when transferred back to normoxic conditions. In addition, we did not notice obvious hydrogel degradation during our short-term in vitro culture period, as shown in Fig. 4(c). All these results correspond to our data in 2D culture, which is promising for further evaluation in vivo. After the demonstration of efficacy of the 30 mM adenosine dose in vivo,, our future studies will include dose responses to evaluate potential increases in efficacy at other doses, or similar efficacy at lower doses. These dosing studies will be important for future clinical translation and Phase I safety studies.

For in vivo characterizations, the design of bioprinted constructs is shown in Fig. 5(a), which is much larger than the design of the in vitro bioprinted model. However, due to the high thickness of bioprinted constructs, cells in the central region of bioprinted constructs should suffer from hypoxia since the diffusion limit of oxygen is only around 200 μm without a vascular structure [6, 30, 31]. The resultant hypoxic in vivo condition in the center of a larger construct is difficult to quantify but is likely to be similar to our previous in vitro hypoxic condition. After two weeks of implantation, both tissue constructs showed minor shrinkage indicating potential degradation behavior of bioprinted constructs

during the long-term in vivo experiment. Moreover, both control and 30 mM AD tissue constructs demonstrate excellent integration with host tissues and vascularization in surrounded bioprinted tissues. The center of bioprinted control tissues responds to in vivo hypoxic conditions by showing disintegrating apoptotic structures as well as the evenly distributed positive staining of HIF1A. However, bioprinted 30 mM AD tissues present cell fusion and little expression of HIF1A in their center indicating the effects of adenosine on reducing cellular mechanism, which increases the cell viability in bioprinted constructs in vivo. In addition, positive desmin staining is observed in the center of bioprinted 30 mM AD tissues indicating muscle cell differentiation for bioprinted 30 mM AD tissues, while bioprinted control tissues present a central disintegrating structure. In the authors' knowledge, this study is the first research attempting to prevent tissue necrosis due to slow vascularization in human-sized bioprinted tissues. The results of this work are promising but have limitations. Future aspects of this study include the incorporation of built-in vascular channels and the human umbilical vein cells to monitor both cell viability, in-depth study of the degradation behavior of bioprinted constructs, and vascular formation within the bioprinted constructs. Additionally, there is potential for this technology to be applied to clinically relevant tissue repair, such as volumetric muscle loss and other skeletal muscle injuries. Our future studies will include functional evaluation of adenosine-containing bioprinted constructs in animal models of skeletal muscle injury. This study takes another path to prevent tissue necrosis in human-sized bioprinted tissues, which is a step forward in overcoming the current challenge of bioprinted tissues toward versatile clinical translations.

## Conclusions

The clinical translation of bioprinted tissues has been a challenge due to slow vascularization leading to tissue necrosis in their center. In this study, adenosine is used to reduce the cellular metabolism for preventing tissue necrosis, which can indirectly achieve more time for tissue vascularization. In vitro results show that the addition of adenosine significantly improves the cell viability and proliferation under hypoxic conditions for 20 and 11 days in 2D and 3D culture, respectively. Cell reproliferation in samples with adenosine is also significantly higher than the control after transferring back to normoxic conditions. In addition, in vivo characterizations indicate that the addition of adenosine can prevent apoptosis and tissue necrosis in the center of bioprinted constructs and support muscle formation. This study shows promising results of using adenosine in bioprinted tissues to improve cell viability and prevent tissue necrosis, which is worth further developing toward clinical translations.

**Acknowledgements** The authors would like to acknowledge the funding from the Armed Forces Institute for Regenerative Medicine (AFIRM) under the grant numbers W81XWH-14-2-0003 and do not have any possible conflict of interest.

**Author contributions** DK was involved in conceptualization, data curation, formal analysis, investigation, methodology, validation, writing—original draft, writing—review & editing and visualization; AMJ helped in writing—review & editing; and SVM, SJL and JJY contributed to funding acquisition, project administration, and supervision.

## Compliance with ethical standards

**Conflict of interest** The authors declare that they have no conflict of interest.

**Ethical approval** This research has been approved by the Animal Care and Use Committee of Wake Forest Institute of Regenerative Medicine.

**Consent to participate** All authors agree to participate in the work related to this article.

**Consent for publication** The manuscript was approved by all authors for publication.

## References

1. Grinyó JM (2013) Why is organ transplantation clinically important? Cold Spring HarbPerspect Med. https://doi.org/10.1101/cshperspect.a014985
2. Organ donation statistics: Why be an organ donor? | organdonor.gov. https://www.organdonor.gov/statistics-stories/statistics.html. Accessed 21 Sep 2017
3. CittadellaVigodarzere G, Mantero S (2014) Skeletal muscle tissue engineering: strategies for volumetric constructs. Front Physiol 5:362. https://doi.org/10.3389/fphys.2014.00362
4. Agostini T, Lazzeri D, Spinelli G (2013) Anterolateral thigh flap: systematic literature review of specific donor-site complications and their management. J Cranio-MaxillofacSurg 41:15–21. https://doi.org/10.1016/j.jcms.2012.05.003
5. Bose S, Ke D, Sahasrabudhe H, Bandyopadhyay A (2018) Additive manufacturing of biomaterials. Prog Mater Sci 93:45–111. https://doi.org/10.1016/j.pmatsci.2017.08.003
6. Ke D, Murphy SV (2018) Current challenges of bioprinted tissues toward clinical translation. Tissue Eng Part B Rev 25:1–13. https://doi.org/10.1089/ten.teb.2018.0132
7. Leberfinger AN, Dinda S, Wu Y et al (2019) Bioprinting functional tissues. ActaBiomater 95:32–49. https://doi.org/10.1016/j.actbio.2019.01.009
8. Cui H, Nowicki M, Fisher JP, Zhang LG (2017) 3D bioprinting for organ regeneration. Adv Healthc Mater 6:1601118. https://doi.org/10.1002/adhm.201601118
9. Izadifar Z, Chang T, Kulyk W et al (2016) Analyzing biological performance of 3D-printed, cell-impregnated hybrid constructs for cartilage tissue engineering. Tissue Eng Part C Methods 22:173–188. https://doi.org/10.1089/ten.TEC.2015.0307
10. Merceron TK, Burt M, Seol Y-J et al (2015) A 3D bioprinted complex structure for engineering the muscle-tendon unit. Biofabrication 7:035003. https://doi.org/10.1088/1758-5090/7/3/035003
11. Park JH, Hong JM, Ju YM et al (2015) A novel tissue-engineered trachea with a mechanical behavior similar to native trachea.

Biomaterials 62:106–115. https://doi.org/10.1016/j.biomaterials.2015.05.008
12. Kang H-W, Lee SJ, Ko IK et al (2016) A 3D bioprinting system to produce human-scale tissue constructs with structural integrity. Nat Biotechnol 34:312–319. https://doi.org/10.1038/nbt.3413
13. Szojka A, Lalh K, Andrews SHJ et al (2017) Biomimetic 3D printed scaffolds for meniscus tissue engineering. Bioprinting 8:1–7. https://doi.org/10.1016/j.bprint.2017.08.001
14. Zhu D, Tong X, Trinh P, Yang F (2018) Mimicking cartilage tissue zonal organization by engineering tissue-scale gradient hydrogels as 3D cell niche. Tissue Eng Part A 24:1–10. https://doi.org/10.1089/ten.tea.2016.0453
15. Ke D, Yi H, Est-Witte S et al (2019) Bioprinted trachea constructs with patient-matched design, mechanical and biological properties. Biofabrication 12:015022. https://doi.org/10.1088/1758-5090/ab5354
16. Choi Y-J, Jun Y-J, Kim DY et al (2019) A 3D cell printed muscle construct with tissue-derived bioink for the treatment of volumetric muscle loss. Biomaterials 206:160–169. https://doi.org/10.1016/j.biomaterials.2019.03.036
17. Moon JJ, West JL (2008) Vascularization of engineered tissues: approaches to promote angio-genesis in biomaterials. Curr Top Med Chem 8:300–310
18. Witzleb E (1989) Functions of the vascular system. Human Physiology. Springer, Berlin, Heidelberg, pp 480–542
19. Daly AC, Freeman FE, Gonzalez-Fernandez T et al (2017) 3D bioprinting for cartilage and osteochondral tissue engineering. Adv Healthc Mater 6:1700298. https://doi.org/10.1002/adhm.201700298
20. Utzinger U, Baggett B, Weiss JA et al (2015) Large-scale time series microscopy of neovessel growth during angiogenesis. Angiogenesis 18:219–232. https://doi.org/10.1007/s10456-015-9461-x
21. Kolesky DB, Homan KA, Skylar-Scott MA, Lewis JA (2016) Three-dimensional bioprinting of thick vascularized tissues. PNAS 113:3179–3184. https://doi.org/10.1073/pnas.1521342113
22. Jakab K, Marga F, Norotte C et al (2010) Tissue engineering by self-assembly and bio-printing of living cells. Biofabrication 2:022001. https://doi.org/10.1088/1758-5082/2/2/022001
23. Kim J, Andersson K-E, Jackson JD et al (2014) Downregulation of metabolic activity increases cell survival under hypoxic conditions: potential applications for tissue engineering. Tissue Eng Part A 20:2265–2272. https://doi.org/10.1089/ten.tea.2013.0637
24. Sheth S, Brito R, Mukherjea D et al (2014) Adenosine receptors: expression, function and regulation. Int J MolSci 15:2024–2052. https://doi.org/10.3390/ijms15022024
25. Buck LT (2004) Adenosine as a signal for ion channel arrest in anoxia-tolerant organisms. Comp BiochemPhysiol B BiochemMolBiol 139:401–414. https://doi.org/10.1016/j.cbpc.2004.04.002
26. Brey EM (2014) Vascularization: regenerative medicine and tissue engineering, 1st edn. CRC Press, Boca Raton
27. Gopinathan J, Noh I (2018) Recent trends in bioinks for 3D printing. Biomater Res 22:11. https://doi.org/10.1186/s40824-018-0122-1
28. Costantini M, Testa S, Mozetic P et al (2017) Microfluidic-enhanced 3D bioprinting of aligned myoblast-laden hydrogels leads to functionally organized myofibers in vitro and in vivo. Biomaterials 131:98–110. https://doi.org/10.1016/j.biomaterials.2017.03.026
29. Kim JH, Seol Y-J, Ko IK et al (2018) 3D bioprinted human skeletal muscle constructs for muscle function restoration. Sci Rep 8:12307. https://doi.org/10.1038/s41598-018-29968-5
30. Brown DA, MacLellan WR, Laks H et al (2007) Analysis of oxygen transport in a diffusion-limited model of engineered heart tissue. BiotechnolBioeng 97:962–975. https://doi.org/10.1002/bit.21295
31. Jain RK, Au P, Tam J et al (2005) Engineering vascularized tissue. Nat Biotechnol 23:821–823. https://doi.org/10.1038/nbt0705-821